Magnetic Interaction between the Tyrosyl Free Radical and the Antiferromagnetically Coupled Iron Center in Ribonucleotide Reductase†

Margareta Sahlin, Leif Petersson, Astrid Gräslund, and Anders Ehrenberg*
Department of Biophysics, Arrhenius Laboratory, University of Stockholm, S-106 91 Stockholm, Sweden

Britt-Marie Sjöberg
Department of Molecular Biology, Biomedical Center, The Swedish University of Agricultural Sciences, S-751 24 Uppsala, Sweden

Lars Thelander‡
Department of Biochemistry, Medical Nobel Institute, Karolinska Institutet, S-104 01 Stockholm, Sweden
Received November 3, 1986; Revised Manuscript Received March 18, 1987

ABSTRACT: Ribonucleotide reductases from *Escherichia coli* and from mammalian cells are heterodimeric enzymes. One of the subunits, in the bacterial enzyme protein B2 and in the mammalian enzyme protein M2, contains iron and a tyrosyl free radical that both are essential for enzyme activity. The iron center in protein B2 is an antiferromagnetically coupled pair of high-spin ferric ions. This study concerns magnetic interaction between the tyrosyl radical and the iron center in the two proteins. Studies of the temperature dependence of electron paramagnetic resonance (EPR) relaxation and line shape reveal significant differences between the free radicals in proteins B2 and M2. The observed temperature-dependent enhanced EPR relaxation and line broadening of the enzyme radicals are furthermore completely different from those of a model UV-induced free radical in tyrosine. The results are discussed in terms of magnetic dipolar as well as exchange interactions between the free radical and the iron center in both proteins. The free radical and the iron center are thus close enough in space to exhibit magnetic interaction. For protein M2 the effects are more pronounced than for protein B2, indicating a stronger magnetic interaction.

The enzyme ribonucleotide reductase catalyzes the reduction of ribonucleotides to their corresponding deoxyribonucleotides. The enzymes coded for in *Escherichia coli*, bacteriophage T4, mammalian cells, and a herpes, pseudorabies, virus all contain iron and a stable tyrosyl free radical necessary for enzyme activity (Thelander & Reichard, 1979; Sjöberg & Gräslund, 1983; Gräslund et al., 1985). The properties of the *E. coli* enzyme have been studied in considerable detail. It consists of two nonidentical subunits, proteins B1 and B2, which form an active 1:1 complex. Protein B1 binds substrate and effector molecules and provides oxidation–reduction active dithiols that participate in the enzyme reaction. Protein B2 consists of two identical polypeptide chains. It contains a dimeric iron center and one stable free radical per homodimeric structure (Ehrenberg & Reichard, 1972; Sjöberg et al., 1978). The amino acid sequence of protein B2 from *E. coli* has been deduced from the nucleotide sequence of its structural gene (Carlsson et al., 1984). It is similar to and may readily be aligned with sequences coding for protein B2 homologues in mouse, herpes simplex virus, Epstein-Barr virus, and bacteriophage T4 (Sjöberg et al., 1985, 1986a; Thelander & Berg, 1986). Conserved areas include the radical residue at Tyr-122 (in *E. coli* numbering) (Larsson & Sjöberg, 1986) and possible ligands of the iron center.

The iron center of protein B2 is an antiferromagnetically coupled pair of high-spin ferric ions, connected by a μ-oxo bridge (Petersson et al., 1980; Atkin et al., 1973; Sjöberg et al., 1982). The presence of the iron center is necessary for the stability of the tyrosyl free radical. The radical and the iron center are formed when radical-free apoprotein reacts with ferrous ions in the presence of oxygen (Petersson et al., 1980; Atkin et al., 1973).

Mammalian ribonucleotide reductase is composed of subunits M1 and M2 corresponding to subunits B1 and B2 of the bacterial enzyme (Engström et al., 1979; Thelander et al., 1985). Protein M2 contains a tyrosyl radical, giving an EPR[1] spectrum that is similar to but not identical with that for the *E. coli* enzyme (Figure 1a,b) (Gräslund et al., 1982). Minor conformational differences in the tyrosyl residues harboring the free radicals can explain these differences (Sahlin et al., 1982). Protein M2 also contains iron (Engström et al., 1979). The iron center of purified protein M2 appears to be of a nature similar to that in protein B2, judged from light absorption spectra (Thelander et al., 1985).

In this study we discuss certain unusual properties of the free radicals of proteins B2 and M2, as observed by EPR. The results include the temperature dependence of the microwave saturation, as well as the EPR line shapes and intensities. Our observations on the EPR relaxation and line shape properties of the free radicals in the *E. coli* and mammalian enzymes may be explained by magnetic interaction between the free radical and the iron center. The latter exhibits an increasing magnetic moment with increasing temperature due to the antiferromagnetic nature of the iron center. Magnetic susceptibility measurements on protein B2 have shown the antiferromagnetic coupling constant to be $-J = 108^{+25}_{-20}$ cm^{-1} (Petersson et al., 1980). A complete quantitative analysis of

† This work was supported by grants from the Swedish Natural Science Research Council and the Swedish Medical Research Council.
‡ *Present address:* Department of Medical Chemistry, University of Umeå, S-901 87 Umeå, Sweden.

[1] Abbreviations: DPPH, α,α'-diphenyl-β-picrylhydrazyl; EDTA, ethylenediaminetetraacetic acid; EPR, electron paramagnetic resonance; Tris, tris(hydroxymethyl)aminomethane.

0006-2960/87/0426-5541$01.50/0

the magnetic interaction between the radical and the iron center is not yet possible for either protein B2 or M2.

Experimental Procedures

Materials. 2′-Amino-2′-deoxy-CDP was a generous gift from Prof. Fritz Eckstein, Max-Planck-Institut für Experimentelle Medizin, Abteilung Chemie, D-3400 Göttingen, West Germany. Azidocytidine from Boehringer Mannheim was phosphorylated to the diphosphate as described by Hobbs et al. (1973). L-[3,5-^{2}H]Tyrosine was a generous gift from Dr. Björn Lindström, National Board of Health and Welfare, Department of Drugs, Uppsala, Sweden (Lindström et al., 1974). ^{57}Fe was obtained from Harwell Stable Isotopes as an Fe foil.

Bacterial Ribonucleotide Reductase. Proteins B1 and B2 were prepared as described earlier (Eriksson et al., 1977). Most of the measurements were performed with two native protein B2 samples, 2.4 and 1.8 mM in protein concentration and 1.5 and 1.2 mM, respectively, in free radical concentration. Specifically deuteriated protein B2 was prepared from cells grown on L-[3,5-^{2}H]tyrosine as described elsewhere (Sjöberg et al., 1977). Some protein B2 samples were obtained by reconstitution of the apoprotein according to Atkin et al. (1973). Apoprotein without both iron and radical was prepared by chelation of the iron in native protein B2 with 8-hydroxyquinoline-5-sulfonate (a saturated solution of the Li salt diluted 10 times). The iron to be introduced into apoprotein B2 was dissolved in 5 M HCl and filtered through glass wool. Its concentration was determined spectrophotometrically. To the iron solution was added 10 molar equiv of ascorbic acid, and the solution was neutralized with Tris base to give pH of 7.6. Reconstitution was obtained in the presence of oxygen by adding a 2 times excess of the iron–ascorbate solution to the apoprotein. In this way ^{57}Fe was introduced into a L-[3,5-^{2}H]tyrosine-substituted apoprotein B2, and a ^{56}Fe sample was made in parallel. The protein concentrations in the reconstituted ^{57}Fe and ^{56}Fe samples were approximately 90 μM, and the radical concentrations were 40 and 50 μM, respectively.

Mammalian Ribonucleotide Reductase. Three different samples were studied: (a) packed cells from hydroxyurea-resistant mouse TA3 cells, overproducing protein M2 and having a protein M2 tyrosyl free radical concentration of about 4 μM (Kjøller Larsen et al., 1982; Thelander et al., 1985); (b) a partially purified ribonucleotide reductase from such cells [protein concentration 11.7 mg/mL in 50 mM Tris-HCl, pH 7.6, and 0.1 M KCl and tyrosyl radical concentration 5.8 μM (Thelander & Gräslund 1983)]; (c) highly purified ribonucleotide reductase from calf thymus, obtained after affinity chromatography on dATP–Sepharose. This material had a specific activity of 25 units/mg and consisted of about 95% protein M1 and 5% protein M2 (total protein concentration 3.5 mg/mL in 50 mM Tris-HCl, pH 7.6, and 0.1 M KCl). To regenerate the tyrosyl free radical the enzyme was incubated in 10 mM dithiothreitol for 10 min at 37 °C before freezing in liquid nitrogen (Thelander et al., 1983). The tyrosyl radical concentration was approximately 0.4 μM.

Model Compound, UV-Induced Tyrosyl Radical. A Philips water-cooled super-high-pressure mercury lamp, SP 500 W, in combination with a UG 5 filter was used to illuminate a 150-μL argon-flushed frozen solution of 10 mM tyrosine in 12.5 mM borate buffer, pH 10.0. The sample, which was contained in an EPR tube and placed in a cold-finger Dewar filled with liquid nitrogen, was illuminated for 1 min, and then the EPR tube was turned 180° and illuminated for an additional 1 min. This procedure resulted in an average tyrosyl radical concentration of approximately 50 μM.

Enzyme Assay. Ribonucleotide reductase activity was determined by measuring the reduction of [^{3}H]CDP as described earlier (Eriksson et al., 1977; Brown et al., 1969). One unit of ribonucleotide reductase activity is defined as the amount of enzyme or subunit in the presence of an excess of the other subunit, which catalyzes the formation of 1 nmol of deoxycytidine diphosphate/min at 25 °C. Protein M2 activity is ribonucleotide reductase activity measured at 37 °C in the presence of saturating amounts of pure calf thymus M1 (Thelander et al., 1980).

Iron Content. Some of the bacterial samples were analyzed by the particle-induced X-ray emission (PIXE) method by Prof. Sven Johansson, Department of Nuclear Physics, Institute of Technology, Lung, Sweden, whose help is gratefully acknowledged. The iron content was consistent with two iron atoms per B2 subunit.

EPR Measurements. EPR first-derivative spectra were usually recorded on a Varian V-4502 X-band (9.5-GHz) EPR spectrometer with a modified microwave bridge including a circulator and a special bias arm. This instrument was equipped with a 100-kHz field modulation, a 6-in. magnet, and a V-4531 multipurpose cavity. Measurements were also performed on a Varian E9 EPR system, equipped with a 9-in. magnet, 100-kHz field modulation, and an E-231 multipurpose cavity. EPR experiments at 77 K were performed with a cold-finger Dewar filled with liquid nitrogen. At temperatures above 77 K the temperature was controlled by flowing nitrogen gas of known temperature past the sample in a Dewar inserted in the cavity. Temperatures below 77 K were achieved with an Oxford Instrument helium-flow cryostat (ESR-9). In this range temperatures were measured with a calibrated gold (0.03% Fe)/chromel thermocouple. Since the thermocouple is not situated at the sample position, temperature gradients in the sample region will result in a difference between the measured temperature and the actual sample temperature. As an independent control the sample temperature was also obtained by means of a Cu–EDTA standard (1 mM Cu^{2+} and 10 mM EDTA) of the same geometry as the samples. A Curie dependence was assumed for its EPR signal amplitude, and 3.6 K was used as a reference point. This temperature was obtained with liquid helium pumped through the cryostat. When differences were observed in the two ways of measurement, the latter method was considered to be reliable. Hence we get an average temperature for the samples. The room temperature spectrum was recorded with a flat cell in a TE-mode cavity.

The incident microwave power read on the attenuator was calibrated with a Hewlett-Packard 431C power meter and/or a Cu–EDTA standard sample (1 mM Cu^{2+} and 10 mM EDTA). At low powers, where the accuracy of the power meter was insufficient, we have estimated the incident power from the EPR signal amplitude of the standard, relying on the fact that it is proportional to $\sqrt{P}$ under nonsaturating conditions. The calibration was performed at 77 K. As a reference point we have used a power that could be read on the meter with high enough accuracy.

Microwave saturation studies were performed in the power range from 10^{-4} mW to 145 mW for the Varian V-4502 X-band spectrometer and in the power range from 10^{-4} mW to 200 mW for the E9 EPR system. Saturation curves were fitted to the theoretical expression by using a nonlinear least-squares fitting program (Derivative Free Non-Linear Regression, BMDP Program Library) run on an AMDAHL computer.

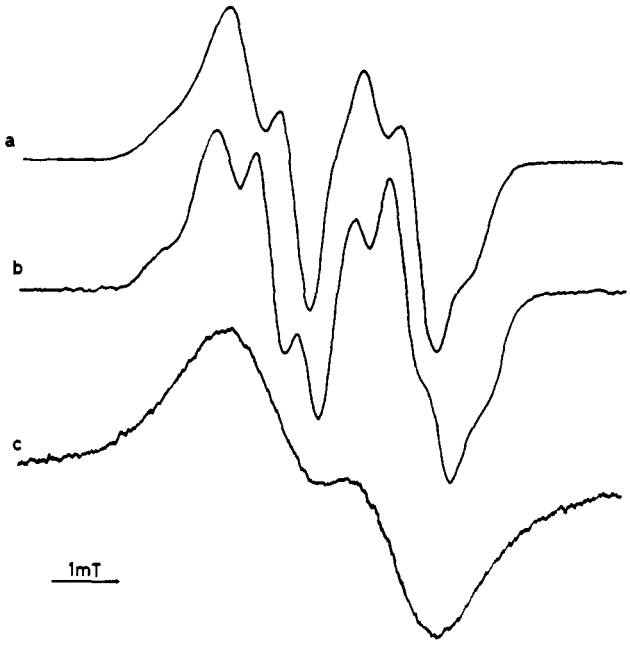

FIGURE 1: EPR spectra of tyrosyl free radical in ribonucleotide reductase from *E. coli* (a) and mouse TA3 cells (b) at 30 K under nonsaturating conditions. Spectrum c shows the EPR spectrum of *E. coli* protein B2 at room temperature under nonsaturating conditions.

The unloaded Q-factor for the different settings of the EPR systems was determined by monitoring the detector leakage as a function of frequency, with the automatic frequency control turned off (Dalal et al., 1981). A readout from a digital voltmeter was used to achieve higher accuracy than that obtained by merely using the readout from the detector leakage current meter of the microwave bridge.

Double integrals of the EPR signals were evaluated by using a computer on-line with the EPR spectrometer. Spin concentrations in the proteins were determined by performing double integrations of the EPR spectra and calibrating at each temperature with a Cu–EDTA standard sample (1 mM Cu^{2+} and 10 mM EDTA).

RESULTS

Microwave Saturation Studies. EPR relaxation was studied through observation of the progressive microwave saturation behavior of the EPR spectra. In order to obtain the temperature dependence of the EPR relaxation, EPR spectra were recorded at various temperatures and microwave power levels for the free radicals in *E. coli* protein B2 and mammalian protein M2. The temperature intervals were chosen as 15–80 K for the B2 radical and 15–40 K for the M2 radical.

Figure 1 shows the low-temperature EPR spectra of the B2 and M2 radicals under nonsaturating conditions (30 K) as well as an EPR spectrum of the B2 radical at room temperature. Figure 2 depicts microwave saturation curves in the form log $X' = \log (Y'/\sqrt{P})/(Y'_0/\sqrt{P_0})$ as a function of log P at three temperatures in the range 20–40 K for the B2 and M2 radicals. Y' is the normalized EPR derivative signal amplitude and P is the microwave power, whereas Y'_0 and P_0 are the corresponding quantities under nonsaturating conditions.

The log X' vs. log P plot gives X' as unity at low microwave powers when no saturation occurs. Figure 2 shows that microwave saturation starts at lower microwave powers in the B2 radical signal than in the M2 one at the same temperature.

The analytical form of microwave saturation curves from EPR derivative signals can be described as

$$X' = (Y'/\sqrt{P})/(Y'_0/\sqrt{P_0}) = 1/(1 + P/P_{1/2})^{b/2} \quad (1)$$

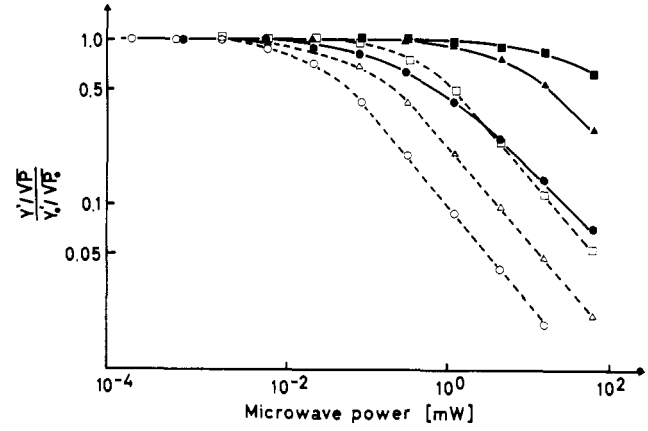

FIGURE 2: Microwave saturating curves of tyrosyl free radical in ribonucleotide reductase from *E. coli* (---) and mouse TA3 cells (—) at 20.0 K (○ and ●), 30.0 K (△ and ▲) and 41.5 K (□ and ■). The vertical axis gives $(Y'/\sqrt{P})/(Y'_0/\sqrt{P_0})$, where Y' is the normalized EPR derivative signal amplitude and P is the microwave power, whereas Y'_0 and P_0 are the corresponding quantities under nonsaturating conditions.

This expression was derived for cases of completely homogeneously broadened (Lorenzian) or completely inhomogeneously broadened (Gaussian) signals, with $b = 3$ or $b = 1$, respectively (Beinert et al., 1967; Ingram, 1958; Poole, 1967; Portis, 1953; Sahlin et al., 1986). In the inhomogeneous case, where the line shape is invariant in all EPR spectra recorded for a saturation curve, the amplitude of the EPR derivative signal is proportional to the EPR absorption.

In both cases, at $P = P_{1/2}$, corresponding to $H_1 = H_{1/2}$, the saturation factor (Ingram, 1958; Poole, 1967; Portis, 1953; Castner, 1959)

$$Z = 1/\left(1 + \frac{1}{4}H_1^2\gamma_f^2T_1T_2\right) \quad (2)$$

is equal to $^1/_2$, i.e.

$$(T_1T_2)^{-1} = \frac{1}{4}\gamma_f^2H_{1/2}^2 \quad (3)$$

Since $H_{1/2}$ is related to $P_{1/2}$ by

$$H_{1/2} = g'\sqrt{QP_{1/2}} \quad (4)$$

the product $(T_1T_2)^{-1}$ at a certain temperature can be determined by evaluating $P_{1/2}$ from the saturation data obtained at that temperature. Here H_1 is the maximum amplitude of the microwave magnetic field at the sample (Portis, 1953; Sahlin et al., 1986) and γ_f is the magnetogyric ratio. T_1 and T_2 are the spin–lattice and spin–spin relaxation times of the free radical, respectively. P is the power given in watts, and Q is the unloaded Q factor of the microwave cavity. The value of Q is in the range 6400–8000 for the different combinations of our EPR systems used.

The value of g' depends on the cavity mode, which in turn depends on the geometry and nature of the sample. To determine g', we have used a DPPH standard having the same geometry as our samples. T_2 for solid DPPH was estimated at room temperature from the peak-to-peak width of its EPR signal. T_1 was supposed to be equal to T_2 at this temperature (Lloyd & Pake, 1953; Brudvig et al., 1984). Equations 3 and 4 with the measured values of $P_{1/2}$ (evaluated as described below), Q, T_1, and T_2 ($T_1 = T_2 \approx 4 \times 10^{-8}$ s) inserted give g' values for the different experimental setups. The g' values determined were 0.045 for the helium-flow cryostat, 0.047 for the cold-finger Dewar, and 0.040 for the Dewar insert used for temperatures above 77 K. An independent determination

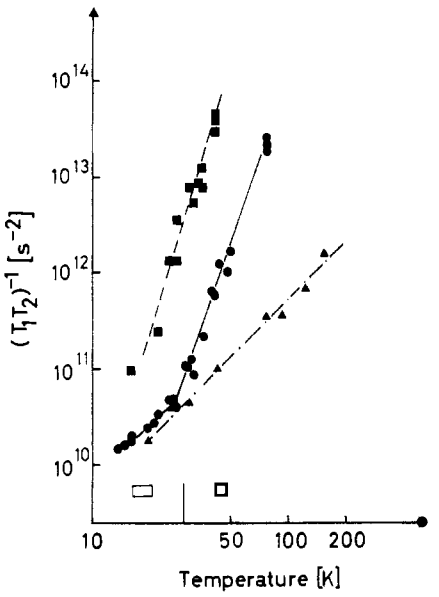

FIGURE 3: Relaxation rate product dependence on temperature for the tyrosyl radical of ribonucleotide reductase from *E. coli* (●) and from mammalian cells (■) and for the UV-induced tyrosyl radical in borate buffer (▲). T_1T_2, the product of the spin–lattice relaxation time T_1 and the spin–spin relaxation time T_2, has been evaluated from the continuous microwave saturation measurements as described in the text. In the measurements, six different samples of B2 and three different samples from mammalian cells, the first two of which originated from TA3 cells and the third from calf thymus, have been used. Measurements were performed on two different EPR spectrometers (see Experimental Procedures). The estimated errors in different temperature regions, <30 K and >30 K, have been indicated by the boxes in the bottom of the figure (see text). In the log–log plot in the case of the mammalian ribonucleotide reductase, there is a slope of 6.7 and the UV-induced tyrosyl radical has a slope of 2.0, calculated by linear regression. For the *E. coli* samples, the line has a slope of 5.7 in the temperature region 28–77 K, also achieved by linear regression.

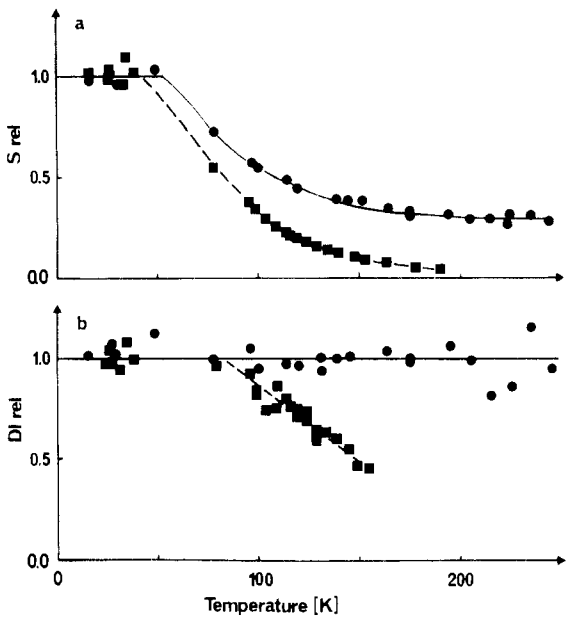

FIGURE 4: Relative EPR absorption derivative amplitude, S_{rel}, and double integral, DI_{rel}, as a function of temperature for the tyrosyl radical of ribonucleotide reductase of *E. coli* (●) and mouse TA3 cells (■). The EPR signals have been corrected for the Curie law temperature dependence. The double integrals were calculated over a magnetic field range of 25 mT. S_{rel} and DI_{rel} have been normalized to unity for their constant low-temperature value.

of g' from the peak-to-peak width of the EPR signal as a function of the circularly polarized microwave magnetic field (Kooser et al., 1969; Rataiczak & Jones, 1972) gave g' values that were ~15% lower than the g' values obtained from determinations based on $P_{1/2}$ values.

By use of a computerized least-squares fitting procedure, all saturation curves for the B2 and M2 radicals at different temperatures were fitted to eq 1 with $P_{1/2}$ and b as adjustable parameters. The b parameter was found to be around 1.3 for the B2 radical and around 1.0 for the M2 radical and the UV-induced tyrosyl radical, indicating a dominant inhomogeneous broadening for all three radicals in the temperature ranges studied. An independent analysis indeed showed that the line shape is very close to a Gaussian one.

The values of $(T_1T_2)^{-1}$ obtained for the B2 and M2 radicals are displayed in Figure 3 as functions of the temperature. For comparison, Figure 3 also shows relaxation data from UV-induced free radicals in tyrosine. The results presented in Figure 3 show that the relaxation rate product of the enzyme radicals of protein B2 above 30 K and of protein M2 at all temperatures where measurements were made is much larger than that of the UV-induced tyrosyl radical. In addition, it is observed that the relaxation is considerably more rapid for the M2 than for the B2 radical.

In Figure 3 the greatest possible errors are indicated as boxes at the bottom of the figure. For the whole temperature region studied, 10–200 K, we estimate the errors from uncertainties in power setting, varying Q factor, and uncertainties in measuring the signal amplitude, to a maximum of ±12% in the product T_1T_2. For the lowest temperatures at about 10 K the uncertainties in temperature determination are estimated to a maximum of ±10%. In the temperature region above 30 K, the relative error in determining the temperature is smaller, ±5%.

Further microwave saturation studies were performed on the mammalian enzyme from different purification steps, containing different proportions of subunits M1 and M2. No significant differences were observed between the samples. Also for the bacterial enzyme the influence of subunit B1 on the relaxation of the radical in subunit B2 was studied in a 1:1 B1–B2 complex. Slightly larger values of $(T_1T_2)^{-1}$ were evaluated for the holoenzyme (data not shown), but the relaxation is still much slower than in the mammalian enzyme. This indicates that the relaxation rates of the radicals are essentially determined by the inherent properties of the iron-containing subunit and only to a minor extent by the interaction with the other subunit. Addition of the substrate analogue amino-CDP (Sjöberg et al., 1983) to the B1–B2 complex had no significant effect on the T_1T_2 parameter (data not shown).

EPR Spectral Shapes and Intensities. The hyperfine patterns of the EPR spectra of the B2 and M2 radicals are best resolved at low temperatures (<30 K; cf Figure 1a,b). At higher temperatures the signals are broadened (Figure 1c). The EPR derivative signal amplitude S_{rel}, obtained under nonsaturating conditions and compensated for the Curie dependence, for both B2 and M2 radicals is independent of temperature below ca. 55 K and at higher temperatures decreases gradually with increasing temperature (Figure 4a). The spectral broadening (vide infra), and the accompanying decrease in S_{rel}, are more pronounced for the M2 radical compared to the B2 radical.

At 77 K the relative signal amplitude has dropped to 70% and 55% of its low-temperature value for the B2 and M2 radicals, respectively. At 150 K the signal amplitude has decreased to 35% for protein B2. Toward higher temperatures it levels off at 30%. The decrease for protein M2 is more pronounced. At 150 K 10% of the signal is left, and the signal

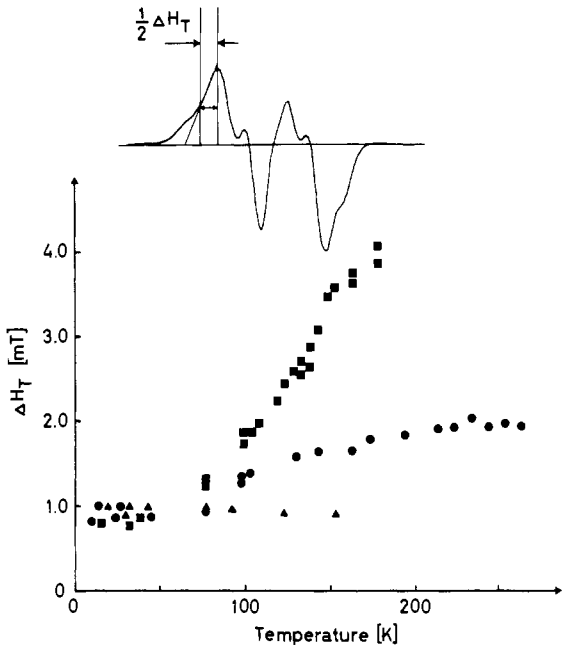

FIGURE 5: Temperature dependences of line width measures of ΔH_T for powder EPR derivative spectra of tyrosyl radicals of ribonucleotide reductase from *E. coli* (●) and mouse TA3 cells (■) and for the model compound, UV-induced tyrosyl radical (▲). EPR spectra were recorded with a field modulation of 10^5 Hz, 0.13–0.16-mT width, and a microwave power not causing saturation. ΔH_T was measured as defined in the inserted spectrum: A triangle was formed by the tangent in the inflection point of the major slope on the low-field side of the spectrum, the vertical line through the maximum point, and the base line. The half-width of this triangle is $^1/_2\Delta H_T$. For lines with pure Gaussian or Lorentzian shape the parameter ΔH_T may be related to the width at half-height of the absorption. It is straightforward to show that $\Delta H_{1/2}(\text{Gauss}) = \{[4\sqrt{2}(\ln 2)^{1/2}]/(3\sqrt{3} - 2)\}\Delta H_T = 1.47\Delta H_T$, and $\Delta H_{1/2}(\text{Lorentz}) = [(2\sqrt{3})/(2\sqrt{3} - 1)]\Delta H_T = 1.41\Delta H_T$.

amplitude continues to decrease at even higher temperature.

Double-integral values DI_{rel} were evaluated (integrated over a magnetic field range of 25 mT) and found to be constant with temperature for the B2 radical. For the M2 radical the double integral was found to decrease significantly with temperature above about 77 K (Figure 4b). At 150 K it had dropped to 45% of its low temperature value. Above this temperature the double-integral values become increasingly uncertain since line broadening effects (Figure 5) result in too low signal amplitudes. An isolated free radical, with a constant value of T_2, i.e., an invariant inherent line shape, should have a constant value of S_{rel} and DI_{rel} independent of temperature when the Curie dependence is compensated for. This behavior was observed for UV-induced tyrosyl free radicals (data not shown).

An estimate of the temperature-dependent line broadening in the radical spectra was obtained by measuring ΔH_T as indicated in the insert of Figure 5. ΔH_T was chosen since this region of the spectrum was observed to have the most "conserved" shape in the first-derivative spectra between the different radicals investigated.

As illustrated in Figure 5, a marked line broadening accompanies the decrease in signal amplitude for the B2 and M2 radicals whereas the line width of the tyrosine model radical appears to be temperature independent. The line broadening is much more pronounced for protein M2 than for protein B2. Thus at 150 K, ΔH_T for the M2 radical is about 4 times its low-temperature (Gaussian) value while for the B2 radical ΔH_T is only doubled.

EPR spectra in the temperature range 4–220 K were also recorded for a B2 protein containing an L-[3,5-^{2}H]tyrosine

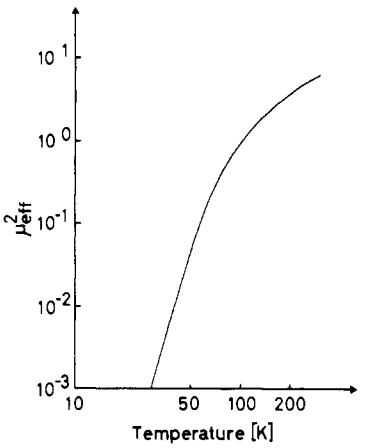

FIGURE 6: The square of the Bohr magneton number, μ_{eff}^2, for the antiferromagnetically coupled iron center in *E. coli* protein B2 as a function of temperature, calculated from the measurements presented in Petersson et al. (1980).

radical with ^{57}Fe ($I = ^1/_2$) instead of ^{56}Fe ($I = 0$) in the binuclear iron center. The aim was to test the possible presence of a hyperfine interaction between the radical and the iron center. Such an interaction might show up as a line broadening after substitution with ^{57}Fe (Tsibris et al., 1968). The deuteriated tyrosine was chosen since it gives a simpler EPR spectrum for the radical, which should facilitate the detection of any line broadening. However, no shape difference at all could be observed between the radical EPR spectra from samples with ^{57}Fe and ^{56}Fe.

DISCUSSION

As seen in Figure 3, the temperature dependences of $(T_1T_2)^{-1}$ are strikingly different for the B2 and M2 radicals and the tyrosyl model radical. For the model radical, log $[(T_1T_2)^{-1}]$ is proportional to log T over the entire temperature range studied, and thus $(T_1T_2)^{-1} \propto T^{\alpha}$. A value of 2.0 is obtained for the exponent α from the slope of the straight line. Below 30 K $(T_1T_2)^{-1}$ values for the B2 and the model radicals are equal within the estimated error limits, while above this temperature $(T_1T_2)^{-1}$ for the B2 radical becomes progressively larger and reflects a more efficient relaxation in this species. We suggest that this can be accounted for by a magnetic interaction between the radical and the iron center. Such an interaction can be of dipolar or exchange origin.

The effect of a magnetic dipolar interaction on the relaxation rate should be a function of the squared effective Bohr magneton number μ_{eff}^2 of the iron center. For protein B2, μ_{eff} can be calculated from previous susceptibility measurements (Petersson et al., 1980) and the temperature dependence of μ_{eff}^2 is shown in Figure 6. Below 30 K, μ_{eff} is very small. It increases rapidly in the temperature region 30–100 K and levels off above 100 K, but here it has already reached a value of approximately 1 μ_B (Bohr magneton). Thus, in the temperature region above 30 K we might expect phenomena arising from magnetic dipolar interaction between the free radical and the iron center, if they are close enough in space. The resulting phenomena should in principle appear in a way similar to those observed, e.g., in cytochrome oxidase (Brudvig et al., 1984) or in spin-labeled biomolecules containing transition metal ions (Eaton & Eaton, 1978). In the present case, however, we might expect a very pronounced temperature dependence of the effects of the interaction because of the temperature-dependent effective magnetic moment.

The electronic ground state of the iron center is diamagnetic, i.e., $S = 0$, due to the antiferromagnetic interaction between

the iron atoms. Considered at a molecular level, the dipolar interaction should take place only in the fraction of molecules where the iron center is in an excited paramagnetic state,i.e., $S > 0$. At the lowest temperatures the population of such states is negligible and the radical behaves as if it is isolated. As the temperature is raised, an increasing fraction of molecules will have their iron center in an excited paramagnetic state. These states can be described by a spin-quantum number S and are $2S + 1$-fold degenerate. Their energies are dependent on the exchange integral J. Thus states with $S = 1, 2, ..., 5$ are found at energies $-2J$, $-6J$, etc. It should be noticed that J is negative in the case of an antiferromagnetic interaction, and thus the multiplets with $S = 1$ and $S = 2$ will be lowest in energy. The J value of -108 cm^{-1}, found for the iron center in protein B2 (Petersson et al., 1980), implies that, in addition to the ground state, essentially only the excited electronic states with $S = 1$ and 2 will be populated in the temperature range studied.

Transitions within the excited spin multiplets or between them and the ground state can give rise to a fluctuating magnetic field at the radical, which will enhance its relaxation rate. If the transition rate between the spin multiplets (of the iron center) T_B^{-1} is slow compared to the radical intrinsic relaxation rate T_{1R}^{-1} the observed values of $(T_1T_2)^{-1}$ (for the radical) should be considered as an average for molecules with their iron centers in different electronic states. If on the other hand the transition rate T_B^{-1} is rapid in comparison to T_{1R}^{-1}, all radicals will experience an iron center with its magnetic moment resulting from an averaging over the different spin multiplets. It should be noted that the iron center will enhance the longitudinal relaxation rate T_1^{-1} of the radical only if the combined rate of transitions between and within the S levels contains frequency components close to the resonance frequency of the radical.

Above 30 K, $(T_1T_2)^{-1}$ for protein B2 is found to vary with temperature as $T^{5.7}$. This temperature dependence should reflect both the temperature-dependent population of the excited states of the iron center (cf. the temperature dependence of μ_{eff}^2) and temperature dependences in T_B^{-1} and T_{1M}^{-1}, where T_{1M}^{-1} denotes the transition rate within the spin multiplets.

An additional explanation for the relaxation properties of the B2 tyrosyl radical could be the presence of a weak exchange interaction between the iron center and the radical. The interaction would result in a mixing of the wave functions of the two spin systems [cf. Colvin et al. (1983)] and would also make spin–lattice relaxation through an Orbach (resonance Raman) process possible. By this mechanism a spin transition within the resulting ground-state doublet proceeds via an excited state (Abragam & Bleaney, 1970). Under the present conditions the effectivity of the Orbach process is expected to be reduced by orders of magnitude (Colvin et al., 1983), and it is conceivable that its rate is comparable to that of a competing Raman process. The result would, however, be a more efficient relaxation for the tyrosyl radical.

The double integral of the EPR signal of protein B2 in Figure 4 is constant over the temperature range studied, indicating that all radical spins are EPR detectable. Above about 55 K a gradually decreasing signal amplitude, Figure 4, and a concomitant signal broadening, Figure 5, are observed with increasing temperature. The broadening is significantly larger than the lifetime broadening, which depends on the spin–lattice relaxation rate of the radical. At 200 K a T_1 value of 0.4 μs was observed for the radical from saturation recovery studies (Sahlin, Ehrenberg, and Hyde, unpublished results). The corresponding lifetime broadening for an individual spin packet may be calculated by means of the relation $\delta H = \hbar/g\beta T_1$ (Bersohn & Baird, 1966; Slichter, 1963) and is found to be less than 0.02 mT. The measured broadening in the powder spectrum of about 1.2 mT at 200 K (cf. Figure 5) obviously demands some other broadening mechanism for a satisfactory explanation. We suggest that also the line broadening effects are mainly a consequence of magnetic interaction between the radical and the iron center. The observed effects are in general agreement with the results predicted by Leigh (1970) from a theoretical analysis of the powder EPR line shape of a spin influenced by dipolar coupling to a second spin in a fixed molecular geometry. A quantitative treatment requires knowledge about the relaxation properties of the spin causing the relaxation, an information that is lacking for the iron center at the present time.

The $(T_1T_2)^{-1}$ values for the tyrosyl radical of the mammalian protein M2 in Figure 3 are significantly larger than for the other species, indicating larger relaxation rates in this case. The temperature dependence of $(T_1T_2)^{-1}$ is proportional to $T^{6.7}$. The decrease in signal amplitude with increasing temperature is more pronounced than for the B2 radical, Figure 4, and it is paralleled by a significantly larger line broadening, Figure 5. If the dipolar interaction model is supposed to be appropriate in this case, such a behavior could be rationalized in several ways. One possibility is that the exchange interaction in the dimeric iron center could be weaker, which would imply smaller energy separations to the excited paramagnetic states and thus result in a larger degree of population for those states than in the B2 case. Different relaxation properties (T_1, T_2) of the electronic spin of the iron center and a smaller distance separation between this center and the tyrosyl radical would also affect the radical relaxation behavior in the observed direction.

A further observation to be considered is that the double integral of the EPR signal from protein M2 decreases continuously above about 70 K while that of protein B2 remains constant. About 45% of the spins are still EPR detectable at the highest temperature studied. This could, at least partly, be a consequence of the large line broadening (Figure 5) for the M2 tyrosyl radical and the limited range of integration. In the most unfavorable case with a pure Lorentzian line shape, the maximum reduction of the double integral should be on the order of 35% at the highest temperature examined, when the field sweep (25 mT), as in our case, is extended to about 6 times the difference in field (4.3 mT) between the peak positions in the first-derivative spectrum (Wertz & Bolton, 1972). An attempt to resolve such a difficulty by extending the sweep range until no reduction in the double integral is seen is, however, not meaningful since imperfections in a base line over a wide sweep range can cause a significant contribution to the double integral.

Even if the chosen sweep range could account for a major part of the decrease in the double integral, there seems to be an additional decrease of about 20% at the highest temperature. A possible qualitative explanation for such a decrease is offered in the work by Leigh (1970), where it is pointed out that dipolar interaction results in an angularly dependent line width. As a consequence, the orientations of some molecules in relation to the applied field may result in such a severe broadening that in practice such molecules do not contribute to the powder EPR spectrum taken over a reasonably limited sweep range.

The radical in protein M2 could also have EPR-silent excited states which are accessible in the temperature range studied. Such states could originate from a weak exchange

interaction between the iron center and the radical. The decreasing double integral would then reflect a depopulation of the radical ground-state doublet. A small change in orientation between the radical and the iron center in protein M2 relative to protein B2 could be sufficient to explain the difference between them. If the interaction is weak compared to the exchange interaction between the iron atoms, the resulting energy levels of the coupled system will be almost the same as those of the iron center but the degeneracy will be doubled. The ground state is a Kramers doublet separated from the first excited state by $-2J$, where J is the exchange integral for the iron center. If J for protein M2 is similar to that of protein B2, the excited states will be thermally accessible in the temperature range examined. A difference with respect to the presence or strength of a weak exchange interaction between the radical and the iron center in proteins B2 and M2 would also contribute to the different relaxation rates for the radical in the two cases.

In case the enhancement of the spin–lattice relaxation rate of the M2 radical makes it larger than that of the B2 radical by a factor of about 10^2, then lifetime broadening would contribute significantly to the observed difference in line width (Figure 5). Taking the results of Figure 3 into account, such a factor is not unreasonable.

In conclusion, our present model of the free radical/iron center in ribonucleotide reductase has the following characteristics: (i) The free radical and the iron center are close enough in space to exhibit magnetic interaction. (ii) The magnetic interaction manifests itself both in a temperature-dependent enhanced spin–lattice relaxation rate and a temperature-dependent increased EPR line width of the enzyme free radical compared to what is expected from an isolated free radical. (iii) For protein M2 the effects are more pronounced than for protein B2, indicating a stronger magnetic interaction.

The proximity between the iron center and the radical demonstrated in this work is in agreement with the conclusion by Thelander et al. (1983) inferred from inhibitor studies and from the fact that radical regeneration from apoprotein takes place in a reaction involving ferrous ions and oxygen (Atkin et al., 1973; Petersson et al., 1980). There is, however, no obvious mechanism by which the iron center directly stabilizes the radical. The tyrosine residue harboring the radical must reside in a pocket in the interior of the protein. This has been suggested from studies using inhibitor analogues with different steric requirements (Kjøller Larsen et al., 1982). Then, once the radical is formed in its protected pocket, its stability may be due to steric hindrance to any one-electron reductants that may be present except those that are known inhibitors, e.g., neutral small molecules such as hydroxylamine and hydroxyurea. Also, the results of a recent resonance Raman study of protein B2 (Sjöberg et al., 1986b) may be of importance in this context. A hydroxide ligand was found to be coordinated to the iron center, and a hydrogen-bonded network was suggested including, the μ-oxo bridge and possibly the phenolic hydroxide of Tyr-122.

REFERENCES

Abragam, A., & Bleaney, B. (1970) *Electron Paramagnetic Resonance of Transition Ions*, p 560, Clarendon, Oxford.

Atkin, C. L., Thelander, L., Reichard, P., & Lang, G. (1973) *J. Biol. Chem. 248*, 7464–7472.

Beinert, H., & Orme-Johnson, W. H. (1967) in *Magnetic Resonance in Biological Systems* (Ehrenberg, A., Malmström, B. G., & Vänngård, T., Eds.) pp 221–247, Pergamon, Oxford.

Bersohn, M., & Baird, J. (1966) *An Introduction to Electron Paramagnetic Resonance*, pp 164–165, Benjamin, New York.

Brown, N. C., Canellakis, Z. N., Lundin, B., Reichard, P., & Thelander, L. (1969) *Eur. J. Biochem. 9*, 561–573.

Brudvig, G. W., Blair, D. F., & Chan, S. I. (1984) *J. Biol. Chem. 259*, 11001–11009.

Carlson, J., Fuchs, J. A., & Messing, J. (1984) *Proc. Natl. Acad. Sci. U.S.A. 81*, 4294–4297.

Castner, T. G., Jr. (1959) *Phys. Rev. 115*, 1506–1515.

Cohn, M., & Reed, G. H. (1982) *Annu. Rev. Biochem. 51*, 365–394.

Colvin, J. T., Rutter, R., Stapelton, H. J., & Hager, L. P. (1983) *Biophys. J. 41*, 105–108.

Dalal, D. P., Eaton, S. S., & Eaton, G. R. (1981) *J. Magn. Reson. 44*, 415–428.

Eaton, S. S., & Eaton, G. R. (1978) *Coord. Chem. Rev. 26*, 207–262.

Ehrenberg, A., & Reichard, P. (1972) *J. Biol. Chem. 247*, 3485–3488.

Engström, Y., Eriksson, S., Thelander, L., & Åkerman, M. (1979) *Biochemistry 18*, 2941–2948.

Eriksson, S., Sjöberg, B.-M., Hahne, S., & Karlström, O. (1977) *J. Biol. Chem. 252*, 6132–6138.

Gräslund, A., Ehrenberg, A., & Thelander, L. (1982) *J. Biol. Chem. 257*, 5711–5715.

Gräslund, A., Sahlin, M., & Sjöberg, B.-M. (1985) *EHP, Environ. Health Perspect. 64*, 139–148.

Hobbs, J., Sternbach, H., Sprinzl, M., & Eckstein, F. (1973) *Biochemistry 12*, 5138–5145.

Ingram, D. J. E. (1958) *Free Radicals as Studied by Electron Spin Resonance*, pp 128–133, Butterworths, London.

Kjøller Larsen, I., Sjöberg, B.-M., & Thelander, L. (1982) *Eur. J. Biochem. 125*, 75–81.

Kooser, R. G., Volland, W. V., & Freed, J. H. (1969) *J. Chem. Phys. 50*, 5243–5257.

Larsson, Å., & Sjöberg, B.-M. (1986) *EMBO J. 5*, 2037–2040.

Leigh, J. S., Jr. (1970) *J. Chem. Phys. 52*, 2608–2612.

Lindström, B., Sjöqvist, B., & Änggård, E. (1974) *J. Labelled Compd. 10*, 187–194.

Lloyd, J. P., & Pake, G. E. (1953) *Phys. Rev. 92*, 1576.

Petersson, L., Gräslund, A., Ehrenberg, A., Sjöberg, B.-M., & Reichard, P. (1980) *J. Biol. Chem. 255*, 6706–6712.

Poole, C. P., Jr. (1967) *Electron Spin Resonance*, pp 695–717, Interscience, New York.

Portis, A. M. (1953) *Phys. Rev. 91*, 1071–1078.

Rataiczak, R. D., & Jones, M. T. (1972) *J. Chem. Phys. 56*, 3898–3911.

Sahlin, M., Gräslund, A., Ehrenberg, A., & Sjöberg, B.-M. (1982) *J. Biol. Chem. 257*, 366–369.

Sahlin, M., Gräslund, A., & Ehrenberg, A. (1986) *J. Magn. Reson. 67*, 135–137.

Sjöberg, B.-M., & Gräslund, A. (1983) *Adv. Inorg. Biochem. 5*, 87–110.

Sjöberg, B.-M., Reichard, P., Gräslund, A., & Ehrenberg, A. (1977) *J. Biol. Chem. 252*, 536–541.

Sjöberg, B.-M., Reichard, P., Gräslund, A., & Ehrenberg, A. (1978) *J. Biol. Chem. 253*, 6863–6865.

Sjöberg, B.-M., Loehr, T. M., & Sanders-Loehr, J. (1982) *Biochemistry 21*, 96–102.

Sjöberg, B.-M., Gräslund, A., & Eckstein, F. (1983) *J. Biol. Chem. 258*, 8060–8067.

Sjöberg, B.-M., Eklund, H., Fuchs, J. A., Carlsson, J., Standart, N. M., Ruderman, J. V., Bray, S. J., & Hunt, T. (1985) *FEBS Lett. 183*, 99–102.

Sjöberg, B.-M., Hahne, S., Mathews, C. Z., Mathews, C. K., Rand, K., & Gait, M. J. (1986a) *EMBO J. 5*, 2031–2036.
Sjöberg, B.-M., Sanders-Loehr, J., & Loehr, T. M. (1986b) *Biochemistry* (submitted for publication).
Slichter, C. P. (1963) *Principles of Magnetic Resonance*, p 155, Harper & Row, New York.
Thelander, L., & Reichard, P. (1979) *Annu. Rev. Biochem. 48*, 133–158.
Thelander, L., & Gräslund, A. (1983) *J. Biol. Chem. 258*, 4063–4066.
Thelander, L., & Berg, P. (1986) *Mol. Cell. Biol.* (in press).
Thelander, L., Eriksson, S., & Åkerman, M. (1980) *J. Biol. Chem. 255*, 7426–7432.
Thelander, L., Gräslund, A., & Thelander, M. (1983) *Biochem. Biophys. Res. Commun. 110*, 859–865.
Thelander, M., Gräslund, A., & Thelander, L. (1985) *J. Biol. Chem. 260*, 2737–2741.
Tsibris, J. C. M., Tsai, R. L., Gunsalus, I. C., Orme-Johnson, W. H., Hansen, R. E., & Beinert, H. (1968) *Proc. Natl. Acad. Sci. U.S.A. 59*, 959–965.
Wertz, J. E., & Bolton, J. R. (1972) *Electron Spin Resonance*, p 464, McGraw-Hill, New York.

Reversible Unfolding of Ribosomal Protein E-L30: An NMR Study†

F. J. M. van de Ven and C. W. Hilbers*
Laboratory of Biophysical Chemistry, University of Nijmegen, Toernooiveld, 6525 ED Nijmegen, The Netherlands
Received November 19, 1986; Revised Manuscript Received April 16, 1987

ABSTRACT: Ribosomal protein E-L30 unfolds reversibly at pH values between 7.0 and 4.5. Unfolding of the protein involves a fast and a slow equilibrium, which depend on the degree of protonation of His_{19} and His_{33}. Both the fast equilibrium between protonated and deprotonated histidines and the slow equilibrium between folded and unfolded protein could be monitored by means of 500-MHz ^1H NMR spectroscopy. The degree of protonation of His_{19} and His_{33} appears to be determinant in the unfolding process of the protein. It is shown however that even when the histidines are uncharged, the protein has only limited stability, probably as a result of the presence of all four Glu's of E-L30 in its triple-stranded β-sheet. At equimolar concentrations of the folded and unfolded form, the rate constant characterizing the transition between these forms is approximately 0.14 s^{-1}. Making use of sequential resonance assignments of the ^1H NMR spectrum [van de Ven, F. J. M., & Hilbers, C. W. (1986) *J. Mol. Biol. 192*, 419–441], the fast equilibrium could be interpreted in terms of alterations in the spatial structure of E-L30 in a specific domain of the molecule. This domain is also affected by temperature although not in exactly the same manner as by pH.

Now that the determination of primary structures of all proteins of the *Escherichia coli* ribosome has been completed (Wittmann, 1982), attention is focusing on the elucidation of the three-dimensional structures of ribosomal proteins (Leyonmarck et al., 1980; Littlechild et al., 1979; Kime et al., 1981; Gudkov et al., 1982; Giri et al., 1979; Appelt et al., 1981, 1983; van de Ven et al., 1983, 1984). The first determination of a spatial structure of a ribosomal component, by means of X-ray crystallography, concerned the C-terminal fragment of protein E-L7/L12 (Leyonmarck et al., 1980). Recently, the spatial structure of the first intact ribosomal protein was successfully investigated by means of X-ray crystallography as well as by NMR. In our laboratory we set out to study the protein E-L30 from the large subunit of the *E. coli* ribosome by means of two-dimensional fourier transform nuclear magnetic resonance (2D FT NMR) (van de Ven et al., 1984; van de Ven & Hilbers, 1986a,b) thereby using strategies mainly developed by K. Wüthrich and collaborators (Nagayama & Wüthrich, 1980; Wagner et al., 1980; Wüthrich et al., 1982; Billiter et al., 1982; Williamson et al., 1984). As a result, we succeeded in obtaining sufficient sequential ^1H NMR resonance assignments and nuclear Overhauser enhancement (NOE) data to present a model for the three-dimensional structure of E-L30 in solution (van de Ven & Hilbers, 1986a,b).

The application of X-ray crystallography for the elucidation of the structures of ribosomal proteins of *E. coli* has been hampered by difficulties in obtaining good crystals (Appelt et al., 1981). However, crystallization has been more successful for ribosomal proteins from *Bacillus stearothermophilus*, and the first structure obtained for these proteins is that of B-L30 of *B. stearothermophilus* (K. S. Wilson, K. Appelt, J. Dijk, I. Tanaka, and S. W. White, personal communication). The proteins E-L30 and B-L30 are 53% homologous (Kimura, 1984), and it was found that the crystal structure of B-L30 and the solution structure of E-L30 are much alike. Moreover, both these proteins appear to be remarkably similar to the C-terminal domain of E-L7/L12 (Leyonmarck et al., 1980) in that they consist of two layers: one layer composed of a triple-stranded antiparallel β-sheet, and one layer composed of two or three antiparallel α-helices.

A major advantage of the application of NMR in protein structural studies is that the folding of these macromolecules can be studied as a dynamic entity (Jardetzky, 1981). Thus, information may be obtained about "ring flipping" of aromatic residues (Campbell et al., 1977), about exchange rates of peptide bond amide protons (Glickson et al., 1969; Wagner & Wüthrich, 1979), about conformational changes relating to biological function (Moonen & Müller, 1984; Ogawa & Shulman, 1972), and about rates and mechanisms of protein folding. In this paper it will be shown that in solution E-L30 is a dynamic system involving multiple forms of the protein in mutual equilibria. The degree of protonation of both histidines in E-L30, His_{19} and His_{33}, appears to be a vital parameter in the equilibrium between folded and unfolded forms of E-L30. A model, which describes the observed phenomena, will be presented.

† This research was supported by the Netherlands Foundation for Chemical Research (SON) with financial aid from the Netherlands Organization for the Advancement of Pure Research (ZWO).

0006-2960/87/0426-5548$01.50/0